

Initial Segment Differentiation Begins During a Critical Window and Is Dependent upon Lumicrine Factors and SRC Proto-Oncogene (SRC) in the Mouse¹

Bingfang Xu, Angela M. Washington, and Barry T. Hinton²

Department of Cell Biology, University of Virginia Health System, Charlottesville, Virginia

ABSTRACT

Without a fully developed and functioning initial segment, the most proximal region of the epididymis, male infertility results. Therefore, it is important to understand the development of the initial segment. During postnatal development of the epididymis, many cellular processes of the initial segment are regulated by lumicrine factors, which are produced by the testis and enter the epididymis with testicular luminal fluid. In this report, we showed that prior to Postnatal Day 15 (P15), the initial segment was lumicrine factor independent in the mouse. However, from P19 onward, lumicrine factors were essential for the proliferation and survival of initial segment epithelial cells. Therefore, P15 to P19 was a critical window that established the dependency of lumicrine factors in the initial segment epithelium. The initial segment-specific kinase activity profile, a marker of initial segment differentiation, was also established during this window. The SFK (SRC proto-oncogene family kinases), ERK pathway (known as the RAF/MEK/ERK pathway) components, and AMPK (AMP-activated protein kinases) pathway components had increased activities from P15 to P19, suggesting that lumicrine factors regulated SFK/ERK/AMPK signaling to initiate differentiation of the initial segment from P15 to P19. Compared with litter mate controls, juvenile *Src* null mice displayed lower levels of MAPK3/1 (mitogen-activated protein kinase 3/1) activity and a reduced level of differentiation in the initial segment epithelium, a similar phenotype resulting from inhibition of SRC activity within the window of P15 to P19. Therefore, lumicrine factor-dependent SRC activity signaling through MAPK3/1 is important for the initiation of initial segment differentiation during a critical window of development.

differentiation, epididymis, ERK pathway, lumicrine regulation, SRC

INTRODUCTION

The mammalian epididymis comprises a single coiled duct, which is about 6 meters long in humans and 1 meter in mice [1]. This long, convoluted epididymal duct provides a luminal fluid microenvironment for sperm maturation, transportation,

¹This work was supported by the Eunice Kennedy Shriver National Institute of Child Health and Human Development/National Institutes of Health grant R01 HD068365 to B.T.H.

²Correspondence: Barry T. Hinton, Department of Cell Biology, University of Virginia Health System, P.O. Box 800732, Charlottesville, VA 22908. E-mail: bth7c@virginia.edu

Received: 6 January 2016.
First decision: 26 January 2016.
Accepted: 20 May 2016.

© 2016 by the Society for the Study of Reproduction, Inc. This article is available under a Creative Commons License 4.0 (Attribution-Non-Commercial), as described at <http://creativecommons.org/licenses/by-nc/4.0>

eISSN: 1529-7268 <http://www.biolreprod.org>
ISSN: 0006-3363

and storage. Without a fully developed and functional epididymis, male infertility will result [2].

The epididymis develops from the anterior part of the Wolffian duct. During embryonic development, the epididymal duct undergoes extensive elongation and coiling [1]. During postnatal development, the epididymis undergoes differentiation and develops into a segmented duct, with each segment having distinct morphological features, gene profile, and functions [2–4]. The most proximal region of the epididymis, the initial segment, must undergo proper differentiation to ensure its function in sperm maturation. *C-ros* oncogene 1 (*Ros1*) knockout male mice that lacked prepubertal differentiation of the initial segment were healthy but infertile. Spermatozoa from *Ros1* null mice showed flagellar angulation, a defect in sperm maturation [5, 6]. Conditional knockout of phosphatase and tension homolog (*Pten*) from the proximal epididymis resulted in dedifferentiation of the initial segment, which in turn resulted in a sperm maturation defect similar to that of *Ros1* knockouts, eventually leading to male infertility [7]. Therefore, it is important to understand the mechanism(s) that regulate(s) initial segment differentiation.

In mice, the period of differentiation of the epididymal epithelium ranges from Postnatal Day 15 (P15) to P44, coincident with the first wave of testicular luminal fluid reaching the epididymis at approximately P15 [8]. Our previous studies showed that lumicrine factors, which enter the epididymis with testicular luminal fluid, stimulated cell proliferation in the initial segment epithelium in juvenile mice and were necessary for epithelial cell survival in adult initial segments [9]. However, it is unclear what the role of lumicrine factors is during initial segment differentiation. We previously reported that lumicrine factors activated MAPK3/1 (mitogen-activated protein kinase 3/1), a marker for initial segment differentiation, in the initial segment epithelium from P15 to P19 and sustained a high level of MAPK3/1 activity in the initial segment onward [9]. Therefore, we hypothesized that lumicrine factors signaled through the ERK pathway (also known as the RAF/MEK/ERK pathway) to regulate initial segment differentiation.

In addition to the higher activity levels of MAPK3/1 in the initial segment compared with other epididymal regions, the differentiated initial segment also has higher activity or gene/protein levels of SRC proto-oncogene family kinases (SFK), PTEN, and the signaling components from the AMP-activated protein kinases (AMPK) pathway [9, 10]. In this report, we investigated the molecular mechanisms initiating differentiation of the initial segment and the role of lumicrine factors and SRC (SRC proto-oncogene), a member of the SFK family, in initial segment differentiation.

MATERIALS AND METHODS

Animals

Mice were handled according to the approved protocols following the guidelines of the Institutional Animal Care and Use Committee of the

TABLE 1. Analysis of the signaling molecule profile during postnatal epididymal development.

Antigens	From P15 to P19	IS versus caput ^a	Localization in epithelial cells	Antibody information	Type of antibody	Working dilution
pSRC Y416	Increase	IS higher	Membrane localization and strong at apical membrane	No. 2101, Cell Signaling Technology	Polyclonal	1:100
pSRC Y527	Decrease	Caput higher	Membrane localization and strong at apical membrane	No. 2105, Cell Signaling Technology	Polyclonal	1:50
SRC	No change	Similar level	Membrane localization and strong at apical membrane	No. 2109, Cell Signaling Technology	Monoclonal	1:100
pRAF1 S259	Decrease	Caput higher	Membrane and cytoplasmic localization and strong near apical membrane	No. 9421, Cell Signaling Technology	Polyclonal	1:100
pMAPK3/1 T202/Y204	Increase	IS higher	Cytoplasmic and nuclear localization	No. 9101, Cell Signaling Technology	Polyclonal	1:200
pRPS6 S235/236	Increase	IS higher	Cytoplasmic localization	No. 4858, Cell Signaling Technology	Monoclonal	1:100
CCND1	Increase	IS higher	Nuclear localization	No. 2978, Cell Signaling Technology	Monoclonal	1:100
AR	No change	Similar level	Nuclear localization	No. SC-13062, Santa Cruz Biotechnology	Polyclonal	1:100
pACC S79	Increase	IS higher	Cytoplasmic and membrane localization	No. 3661, Cell Signaling Technology	Polyclonal	1:100
ACC	Increase	IS higher	Cytoplasmic and membrane localization	No. 3676, Cell Signaling Technology	Monoclonal	1:50
pAMPK β 1/2 S108	Increase and localization change	IS higher	Nuclear and membrane localization	No. 4181, Cell Signaling Technology	Polyclonal	1:100
AMPK β 1/2	Increase	IS higher	Cytoplasmic, nuclear and membrane localization	No. 4150, Cell Signaling Technology	Monoclonal	1:50
pEGFR Y1045	No change	IS higher at P28	Membrane localization at apical membrane	No. 2237, Cell Signaling Technology	Polyclonal	1:50
pMET T1234/1235	No change	IS higher at P28	Membrane localization at apical membrane	No. 3077, Cell Signaling Technology	Monoclonal	1:75
PTEN	No change	IS higher at P28	Cytoplasmic, nuclear, and membrane localization and strong near apical membrane	No. 138G6, Cell Signaling Technology	Monoclonal	1:200

^aIS, initial segment.

University of Virginia. *Src* null mice were reported on previously [11, 12]. Mice were bred and genotyped according to the protocols published by The Jackson Laboratory (Bar Harbor, ME).

We defined epididymal regions according to previous studies [3], which divided the epididymis into either 4 major regions or 10 more defined regions: initial segment (I–II), caput (III–VI), corpus (VII–VIII), and cauda (IX–X). The illustration of initial segment regions I, II, and III was shown in a previous study [7].

Efferent Duct Ligation

To block lumicrine factors from reaching the epididymis, unilateral efferent duct ligation (EDL) surgeries were performed using the protocol modified from the rat EDL procedure, which was described previously in detail [9, 13]. Great care was taken to avoid ligating nearby blood vessels. For the control, a sham operation was performed on the contralateral side within the same animal. Pentobarbital sodium injection (50 mg/kg of body weight) was used as the anesthesia during the surgery. Twenty-four hours or 1 wk after EDL, mice were euthanized by Isothesia (isoflurane) gas overdose followed by cervical dislocation. The tissues were harvested and processed for immunofluorescence analysis.

Immunofluorescence

To examine protein levels during a time course of epididymal development, the epididymides from P15 to P28 were collected from the mice belonging to the same litter, to minimize developmental differences between different litters. Epididymal tissue samples were immersion fixed in 4% paraformaldehyde in PBS overnight at 4°C. Subsequently, the epididymides from different time points were positioned, side by side, and pre-embedded in 1% agarose in a single block. Overall, samples were collected from four litters, and four sets of biological replicates were generated. Similarly, the epididymides from littermate control and knockout mice or inhibitor-treated mice were paired and pre-embedded in agarose block, and sample replicates were generated.

Then, agarose pre-embedded samples underwent paraffin embedding and sectioning, tissue sections were placed on slides, and slides were deparaffinized and rehydrated. For antigen retrieval, slides were microwaved in antigen unmasking solution (Vector Laboratories, Burlingame, CA) for 10 min on high in a 1300-W microwave and cooled for 1 h at room temperature. Following immersion in blocking solution with 10% (v/v) normal goat serum (Vector Laboratories), 0.5% (v/v) gelatin from cold-water fish skin (Sigma, St. Louis, MO), and Tris-buffered saline (TBS) for 1.5 h, slides were incubated overnight at 4°C in blocking solution with primary antibodies. Following washing in TBS, slides were incubated with a 1:200 dilution of Alexa Fluor 594 secondary antibodies (Molecular Probes, Eugene, OR) in blocking solution for 1.5 h at room temperature. All slides were washed in TBS and mounted using Prolong Anti-fade reagent with 4',6-diamidino-2-phenylindole (DAPI) for nuclear

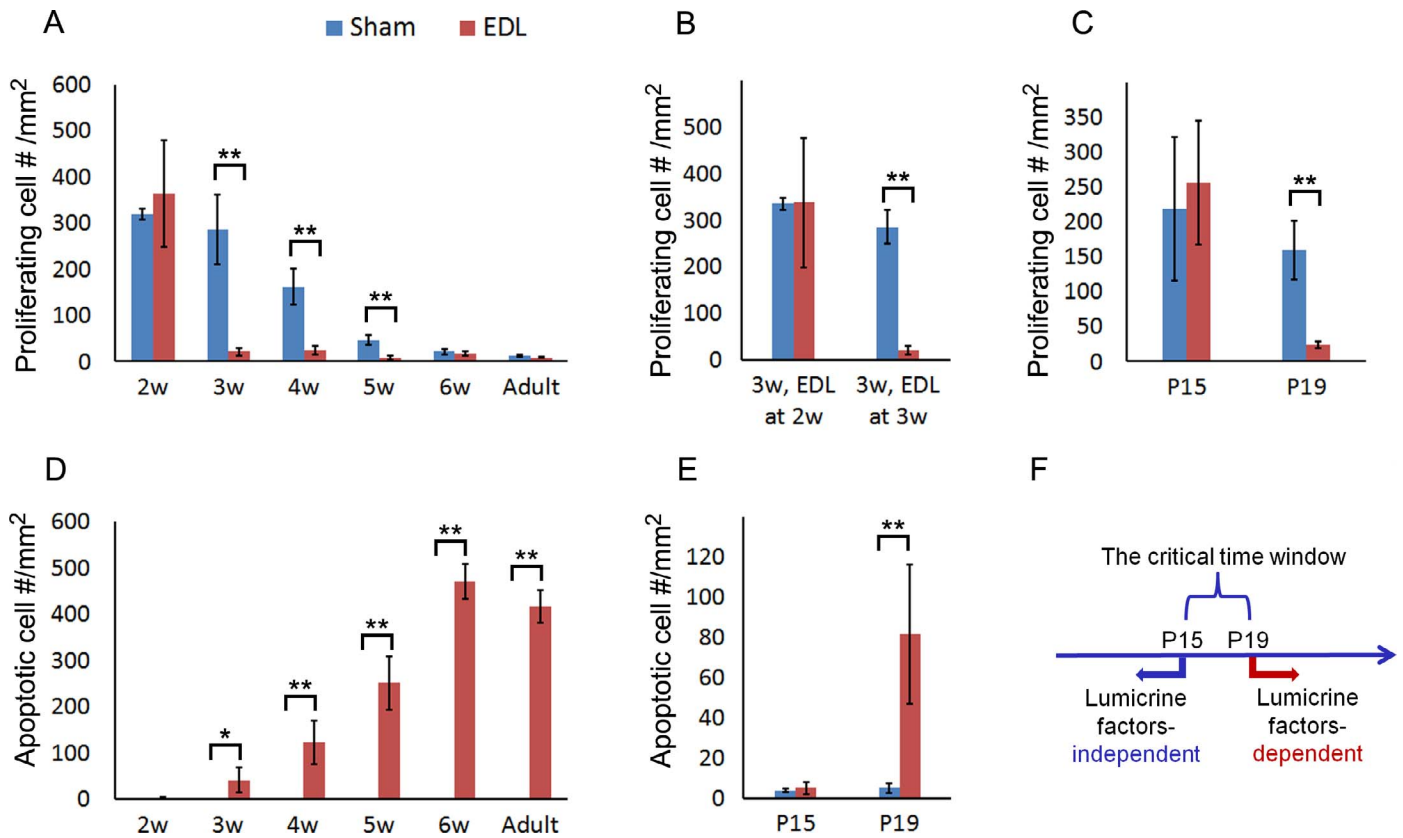


FIG. 1. Lumicrine factor dependency of the initial segment epithelium. **A)** Measurement of cell proliferation in the initial segment after 24 h of EDL, which was performed from the ages of 2 wk to adult. **B)** Measurement of cell proliferation at the age of 3 wk after 1 wk or 24 h of EDL, which was performed at the ages of either 2 wk or 3 wk, respectively. **C)** Measurement of cell proliferation after 24 h of EDL, which was performed at P15 and P19, respectively. **D)** Measurement of apoptosis in the initial segment after 24 h of EDL, which was performed from the ages of 2 wk to adult. **E)** Measurement of apoptosis after 24 h of EDL, which was performed at P15 and P19, respectively. **F)** A diagram shows that P15 to P19 is a critical window for the initial segment epithelium to establish lumicrine factor dependence during postnatal development. Cell proliferation was measured by counting p-Histone H3-positive cells per epididymal area. Apoptosis was measured by counting cleaved-Caspase3-positive cells per epididymal area. Data shown are mean \pm SEM, $n \geq 3$. ****** $P < 0.01$ versus sham; ***** $P < 0.05$ versus sham.

staining (Molecular Probes) and viewed under a Zeiss microscope equipped with epifluorescence. If different labeling patterns were found between two epididymal regions, images were taken across two regions. If not, images were taken at the center of the individual region. For each primary antibody, immunofluorescence experiments were repeated at least three times on different sample replicates. Primary antibodies used in this study are listed in Table 1. In addition, phospho-Histone H3 antibody (no. 06-570; 1:500 working dilution) was purchased from Millipore (Billerica, MA). Cleaved-caspase3 antibody (no. 9661; 1:100 working dilution) and normal rabbit immunoglobulin G (IgG; no. 3900, 1:50 working dilution) were from Cell Signaling Technology (Beverly, MA).

To ensure that labeling intensity was comparable among images, each panel of images was taken from the same slide, which contained a serial of tissue sections. When measuring labeling intensity of membranes and nuclei, lines across/along membranes or across several nuclei were drawn, and labeling intensity along the line was measured using ImageJ Plot Profile and normalized to the length of the line. For each image, at least three lines were measured from different cross sections of the epididymal duct, and the average was calculated. When measuring labeling intensity of the cytoplasm, a small square was drawn, and labeling intensity within the square was measured using the ImageJ Histogram function. The same fixed square was then moved to another cytoplasmic location for measurement. For each image, at least three squares were measured from different cross sections of the epididymal duct, and the average was calculated. For each antibody, labeling intensity was measured on three or more panels of images. If the results from multiple panels were consistent, representative image panels and quantification data were reported.

Measurement of Cell Proliferation and Apoptosis

Immunofluorescence experiments were performed to label proliferating and apoptotic cells using phospho-Histone H3 antibody (no. 06-570; 1:500 working

dilution) and cleaved-CASP3 antibody (no. 9661; 1:100 working dilution), respectively. Cell proliferation was measured by manually counting the number of p-Histone H3-positive cells per mm² epithelial area. Apoptosis was measured by manually counting cleaved-Caspase3-positive cells per mm² epididymal area and epididymal area were measured using Image-Pro Plus software (Media Cybernetics, Silver Spring, MD).

Inhibitor Injection

A daily dose of Bosutinib (LC Laboratories, Woburn, MA) was administered intraperitoneally to wild-type C57B6 mice from P15 to P19 at 30 mg/kg of body weight, and the tissues were harvested at P19 and processed for immunofluorescence analysis.

Statistics

One-way analysis of variance was performed to identify significant changes between groups. The significant difference was indicated by ***P < 0.05** and ****P < 0.01**. Area was measured using Image-Pro Plus (Media Cybernetics, Rockville, MD) and ImageJ software (<http://www.imagej.nih.gov>).

RESULTS

The Initial Segment Established Dependence on Lumicrine Factors from P15 to P19

In this study, EDL was performed at different ages to examine the roles of lumicrine factors during development of the initial segment. As shown in Figure 1A, deprivation of lumicrine factors for 24 h resulted in a significant decline in the

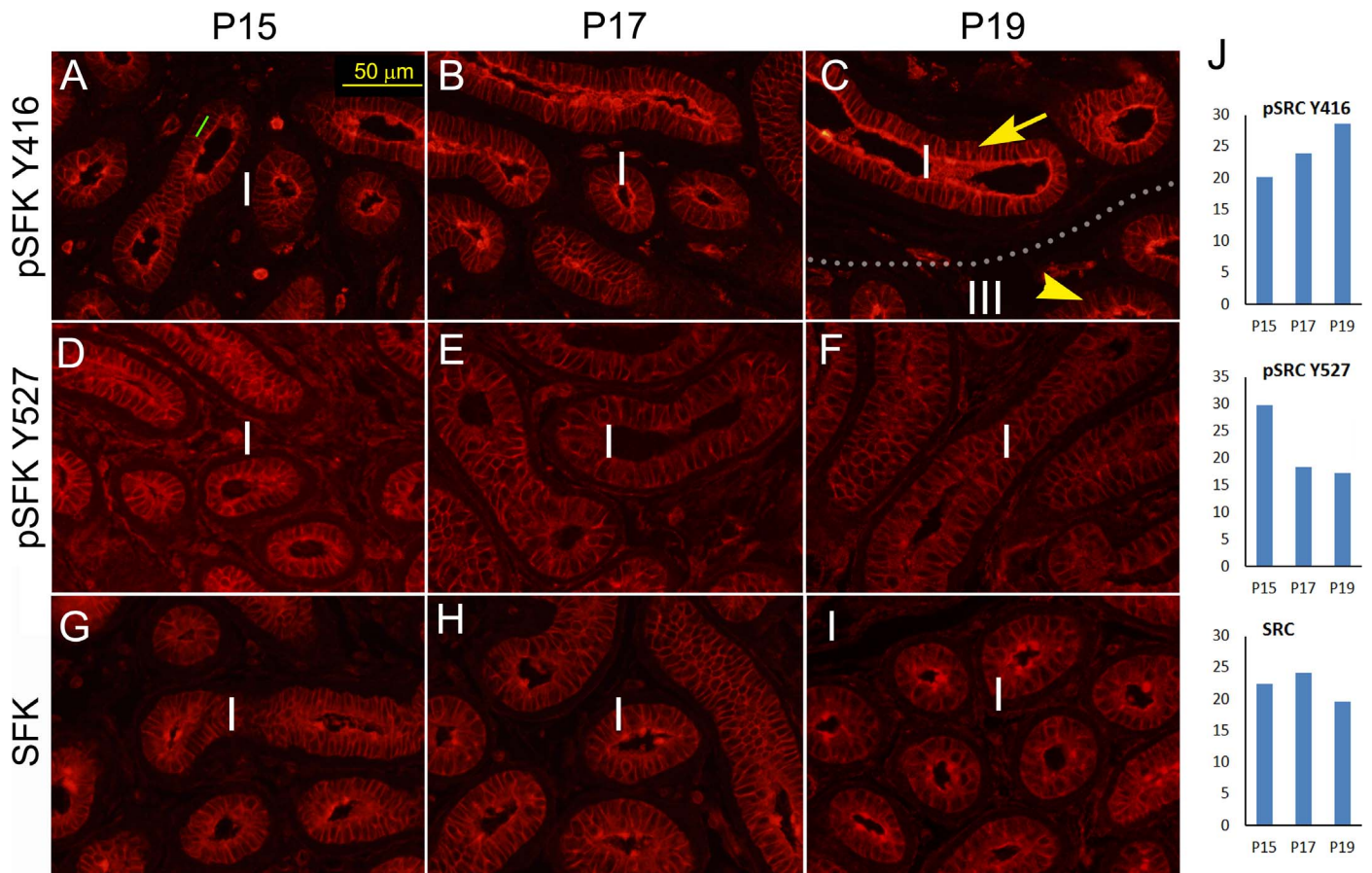


FIG. 2. Activation of SFK from P15 to P19 in the initial segment. **A–C**) A representative panel of images showing the levels of SFK phosphorylated at Y416, an activation site, from P15 to P19 in regions I and III. A dotted line shows the border between regions I and III. An arrow and an arrowhead show labeling of phospho-SFK at Y416 at the basolateral membrane of epithelial cells at P19 in regions I and III, respectively. A line across basolateral membranes at the midway point from apical to basal ends of epithelial cells represents the lines used to quantify labeling intensity. **D–F**) A representative panel of images showing the levels of SFK phosphorylated at Y527, an inhibitory site, in region I from P15 to P19. **G–I**) A representative panel of images showing total SFK protein levels in region I from P15 to P19. **J**) Quantification of labeling intensity of phospho-SRC Y416, phospho-SRC Y527, and total SRC at the basolateral membrane from P15 to P19. Each panel of images was taken from the same slide, which contained tissue sections from P15 to P19. Labeling intensity along the lines across the basolateral membrane of epithelial cells was measured using ImageJ Plot Profile and was shown in arbitrary units.

proliferation of epithelial cells from the ages of 3 to 5 wk. However, high levels of proliferation of epithelial cells at the age of 2 wk were not affected by 24-h EDL. For 3-wk-old mice, when EDL was performed at 2 wk, proliferation in the initial segment epithelium of EDL groups was comparable to sham controls a week later at the age of 3 wk. In contrast, when EDL was performed at 3 wk, proliferation declined significantly 24 h later compared with controls also at the age of 3 wk (Fig. 1B). In addition, 24-h EDL was performed on different days between 2 and 3 wk. As shown in Figure 1C, EDL did not affect cell proliferation at P15. However, deprivation of lumicrine factors resulted in a significant decline in proliferation of epithelial cells at P19 (Fig. 1C).

Deprivation of lumicrine factors for 24 h also resulted in apoptosis in the initial segment epithelium from the age of 3 wk onward. However, EDL did not result in apoptosis at the age of 2 wk (Fig. 1D). More precisely, prior to P15, deprivation of lumicrine factors did not result in apoptosis in the initial segment. Only from P19 onward did it result in apoptosis in the initial segment epithelium (Fig. 1E).

As shown in Figure 1F, prior to P15, epithelial cells in the initial segment were lumicrine factor independent; from P19 onward, they relied on lumicrine factors for proliferation and survival.

The Initial Segment Established Its Distinct Kinase Profile from P15 to P19

We previously reported a list of protein kinases that had specific activities in the initial segment compared with the caput [9]. To investigate which kinase(s) was/were involved in cellular processes from P15 to P19, the changes of these kinases in protein and/or activity levels were analyzed during this critical time window.

SFK activity is regulated by tyrosine phosphorylation at two sites, with opposing effects. Phosphorylation of Y416 in the activation loop of the kinase domain upregulates enzyme activity. Phosphorylation of Y527 in the carboxy-terminal tail by cSRC tyrosine kinase (CSK) renders the enzyme less active [14]. Phospho-SFK and total SFK were localized to the plasma membrane. The levels of SFK phosphorylated at the activation site Y416 increased from P15 to P19 (Fig. 2, A–C and J). Stronger labeling at the basolateral membrane was observed in region I at P19 compared with region III or earlier time points of region I (Fig. 2, A–C, arrow and arrowhead). The phosphorylation levels of SFK at Y527, the inhibitory site, decreased from P15 to P19 (Fig. 2, D–F and J) in region I. Total protein levels of SFK did not change during the same time window in region I (Fig. 2, G–J).

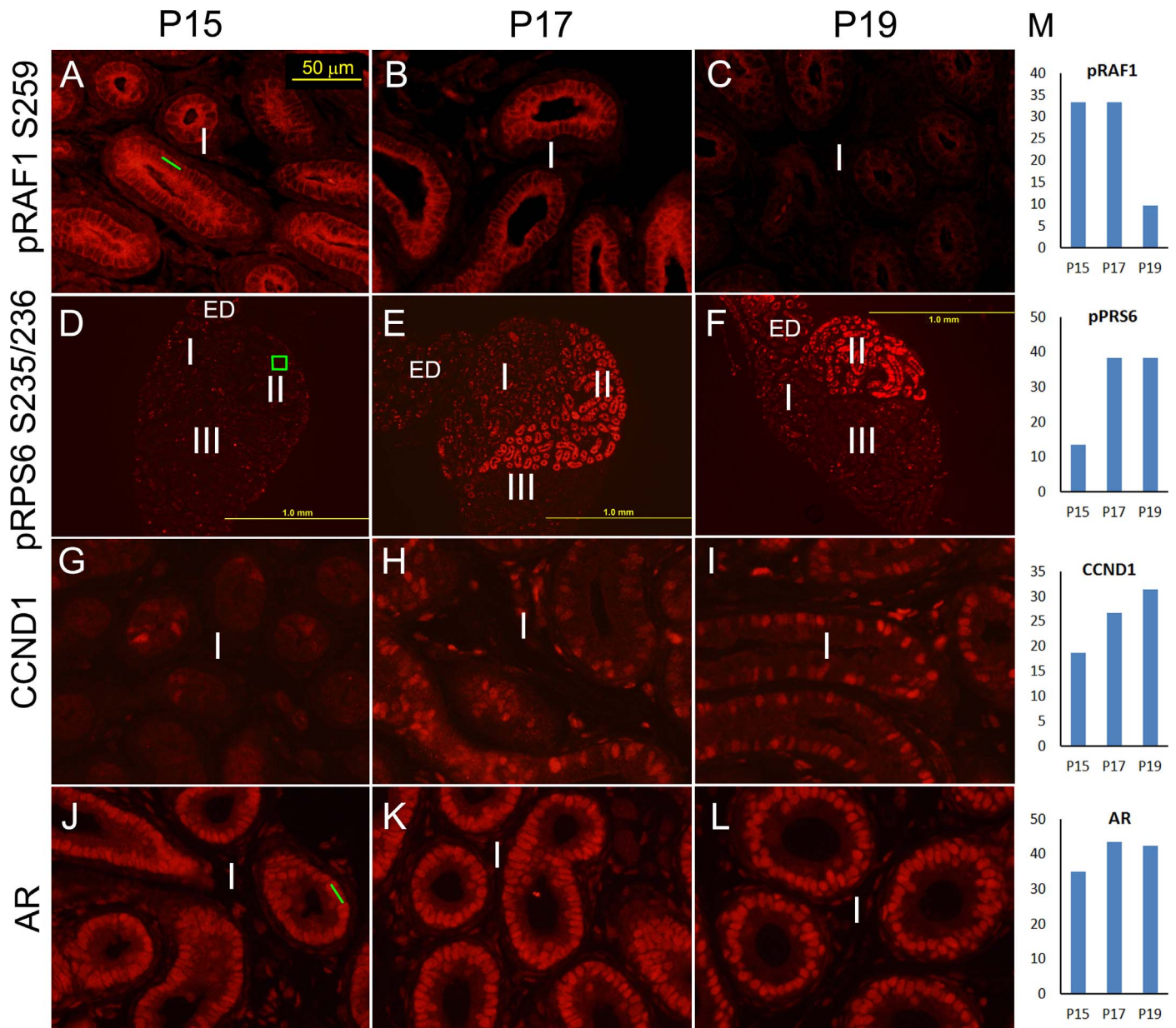


FIG. 3. Phosphorylation or protein levels of RAF1, RPS6, CCND1, and AR from P15 to P19 in the initial segment. **A–C**) A representative panel of images showing the levels of RAF1 phosphorylated at S259 in region I from P15 to P19. A line across basolateral membranes at the midway point from the apical to the basal ends of epithelial cells represents the lines used to quantify labeling intensity. **D–F**) A representative panel of images showing the levels of RPS6 phosphorylated at S235/236 in regions I, II, and III from P15 to P19. ED: efferent ducts. A square at region II represents the squares used to quantify labeling intensity. **G–I**) A representative panel of images showing the protein levels of CCND1 in region I from P15 to P19. **J–L**) A representative panel of images showing the protein levels of AR in region I from P15 to P19. A line across multiple nuclei represents the lines used to quantify labeling intensity. **M**) Quantification of labeling intensity of phospho-RAF1 at the basolateral membrane, phospho-RPS6 in region II, CCND1, and AR in the nuclei from P15 to P19. Each panel of images was taken from the same slide, which contained tissue sections from P15 to P19. Labeling intensity along the lines or within the squares was measured using ImageJ Plot Profile or ImageJ Histogram function, respectively, and it was shown in arbitrary units.

RAF1 (RAF1 proto-oncogene) phosphorylated at S259 was localized to the subcellular region near and/or at the apical membrane and the basolateral membrane of epithelial cells. The levels of immunolabeling of RAF1 phosphorylated at S259, an inhibitory site, decreased from P15 to P19 (Fig. 3, A–C and M) in region I. RPS6 (ribosomal protein S6) phosphorylated at S235/236 had cytoplasmic localization. Phospho-RPS6 levels increased in regions I and II from P15 to P19 (Fig. 3, D–F and M). Compared with region I, region II had a higher level of immunolabeling of phospho-RPS6 at P17 and P19 (Fig. 3, D–F). CCND1 (cyclin D1), which was found to be a downstream target of the ERK pathway in the initial

segment [9], showed a checkerboard labeling pattern in the nuclei. From P15 to P19, an increased number of epithelial cells showed positive labeling in the nuclei in region I (Fig. 3, G–I). Androgen receptor (AR), the expression level of which correlates with the genomic regulation of androgen, was localized to the nuclei, and labeling intensity did not change from P15 to P19 in region I (Fig. 3, J–M).

AMPK β 1/2 phosphorylated at S108 showed nuclear and basolateral membrane localization. Labeling intensity increased at the basolateral membrane from P15 to P19 in region I. At P19, basolateral membrane labeling was distinctly higher in region I compared with region III (Fig. 4, A–C and M, arrow

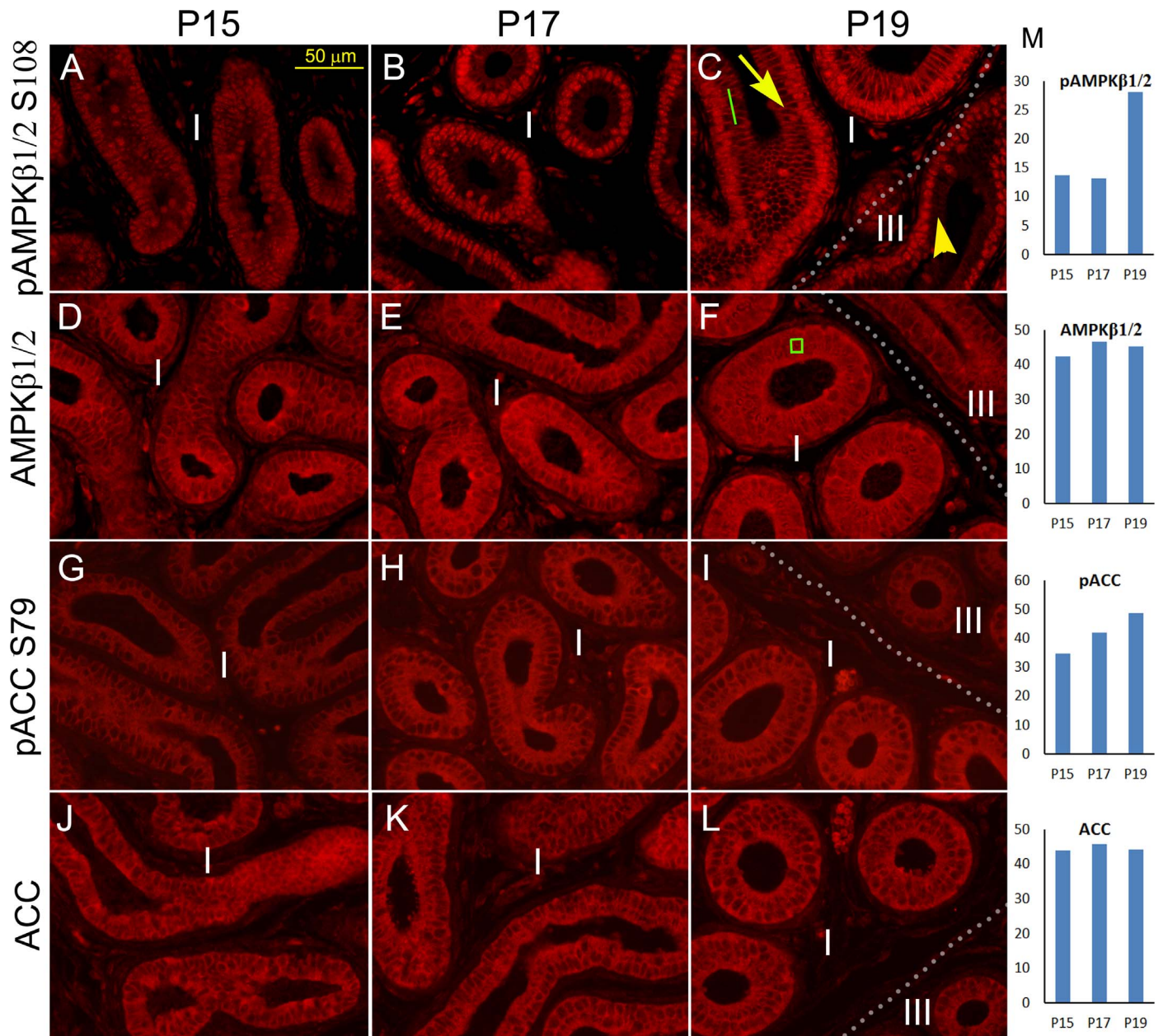


FIG. 4. Activation of the AMPK pathway components from P15 to P19 in the initial segment. **A–C** A representative panel of images showing the levels of AMPKβ1/2 phosphorylated at S108 in regions I and III from P15 to P19. An arrow and an arrowhead show phospho-AMPKβ1/2 labeling at the basolateral membrane of epithelial cells at P19 in regions I and III, respectively. A line across basolateral membranes at the midway point from the apical to the basal ends of epithelial cells represents the lines used to quantify labeling intensity. **D–F** A representative panel of images showing the protein levels of AMPKβ1/2 in region I and III from P15 to P19. A square in the cytoplasmic area represents the squares used to quantify labeling intensity. **G–I** A representative panel of images showing the levels of ACC phosphorylated at S79 in regions I and III from P15 to P19. **J–L** A representative panel of images showing the protein levels of ACC from P15 to P19 in regions I and III. **M** Quantification of labeling intensity of phospho-AMPKβ1/2 at the basolateral membrane, AMPKβ1/2, phospho-ACC, and ACC in the cytoplasm from P15 to P19. The dotted lines show the border between regions I and III. Each panel of images was taken from the same slide, which contained tissue sections from P15 to P19. Labeling intensity along the lines or within the squares was measured using ImageJ Plot Profile or ImageJ Histogram function, respectively, and it was shown in arbitrary units.

and arrowhead). Total protein AMPKβ1/2 had a broad localization pattern. It was localized to the cytoplasm and also on the plasma membrane and in the nuclei. AMPKβ1/2 protein levels increased from P15 to P19 in region I. A higher level of AMPKβ1/2 in region I compared with region III was observed at P19 (Fig. 4, D–F and M). Both acetyl-CoA carboxylase (ACC) phosphorylated at S79 and total ACC protein had plasma membrane and cytoplasmic localization. The levels of ACC phosphorylated at S79 increased from P15 to P19 in region I. At P19, a higher labeling intensity of phospho-ACC in

region I compared with region III was observed (Fig. 4, G–I and M). Labeling intensity of total ACC protein at the cell membrane and cytoplasm did not change from P15 to P19 (Fig. 4, J–M) in region I.

Some differentially expressed or activated proteins between the initial segment and the caput did not show changes in protein and activity levels from P15 to P19. Epidermal growth factor receptor (EGFR) phosphorylated at Y1045 and MET (MET proto-oncogene) phosphorylated at T1234/1235 had a weak and broad localization pattern, and the pattern did not

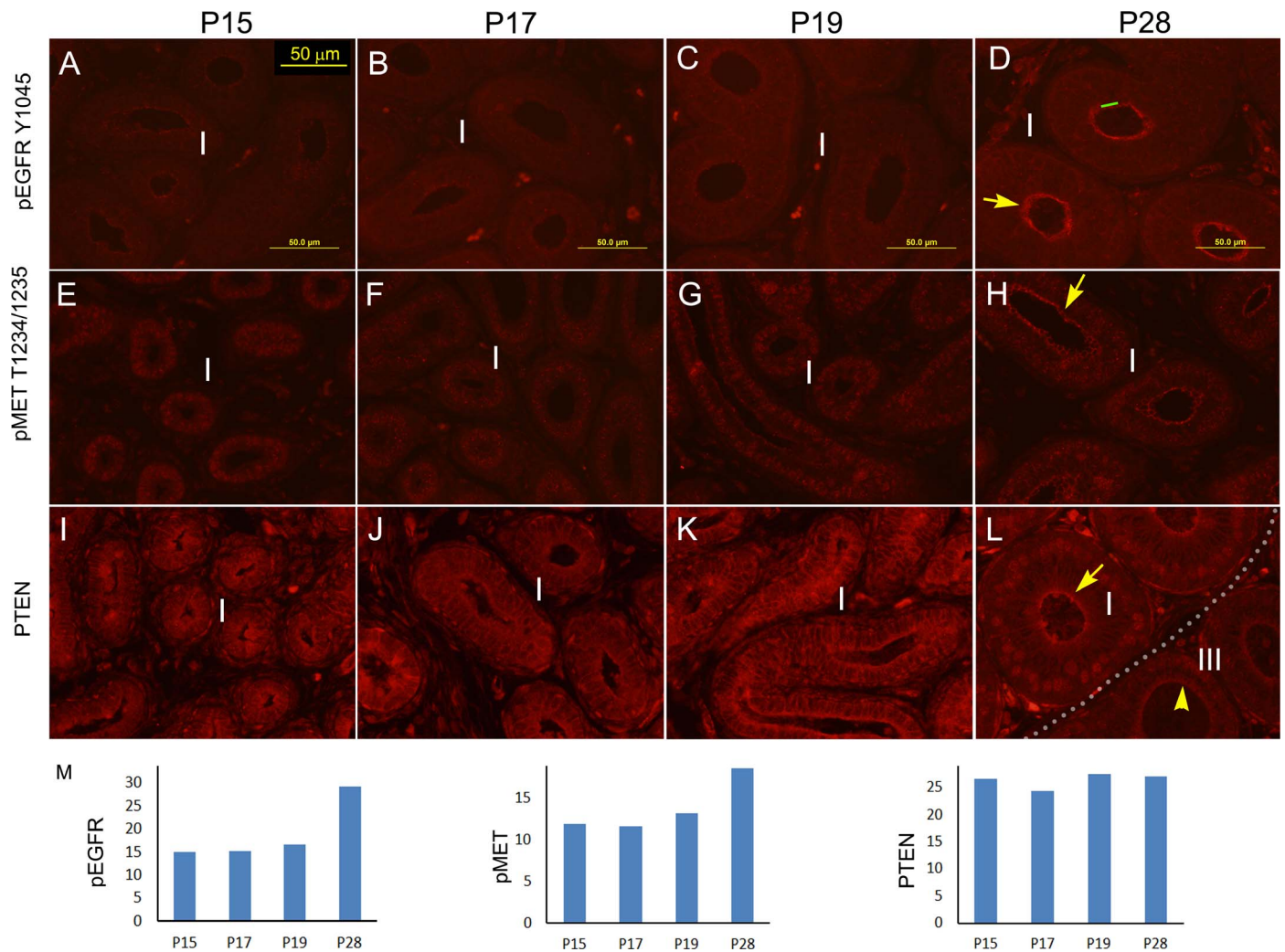


FIG. 5. Phosphorylation or protein levels of EGFR, MET, and PTEN from P15 to P28 in the initial segment. **A–D**) A representative panel of images showing the levels of EGFR phosphorylated at Y1045 in region I from P15 to P28. A line along the apical membrane represents the lines used to quantify labeling intensity. An arrow shows the labeling of phospho-EGFR at/near the apical membrane at P28. **E–H**) A representative panel of images showing the levels of MET phosphorylated at T1234/1235 in region I from P15 to P28. An arrow shows the labeling of phospho-MET at/near the apical membrane at P28. **I–L**) A representative panel of images showing the protein levels of PTEN in regions I and III from P15 to P28. An arrow and an arrowhead show the PTEN labeling at/near the apical membrane at P28 in regions I and III, respectively. **M**) Quantification of labeling intensity of phospho-EGFR, phospho-MET, and PTEN at the apical membrane from P15 to P28. The dotted line shows the border between regions I and III. Each panel of images was taken from the same slide, which contained tissue sections from P15 to P28. Labeling intensity along the lines was measured using ImageJ Plot Profile and was shown in arbitrary units.

change from P15 to P19. However, at P28, specific labeling of phospho-EGFR and phospho-MET adjacent to the apical membrane was found in region I (Fig. 5, A–H and M, arrows). PTEN was localized to the cytoplasm and on the plasma membrane and was concentrated to the subcellular region near and/or at the apical membrane of epithelial cells. The localization pattern did not change from P15 to P19 in the initial segment. At P28, PTEN labeling near the apical membrane remained unchanged from P15 and P19 (Fig. 5M). However, it was higher in epididymal region I compared with region III (Fig. 5L, arrow and arrowhead), whereas nuclear localization of PTEN was observed in region I but not in region III (Fig. 5L). Control images of immunofluorescence labeling using normal rabbit IgG or secondary antibody alone are shown in Supplemental Figure S1 (available online at www.bioreprod.org).

Loss of Src Affected Initial Segment Differentiation as Measured by Changes in Phospho-MAPK3/1

Src null mice suffered from osteopetrosis [11], which resulted in failure of tooth eruption, and the mice needed special diet supplements to avoid malnutrition after weaning. To avoid any health issues, we focused our study on preweaned P17 mice. More importantly, P17 is in the middle of the critical time window of initiation of initial segment differentiation.

The body weight of P17 *Src* null mice (*Src*^{-/-}; 9.2 ± 0.2 g) was not significantly different from controls (*Src*^{+/+} and *Src*^{+/-}; 10.0 ± 0.8 g). The testis width and length of P17 *Src* null mice were 30.0 ± 0.7 mm and 44.1 ± 0.8 mm, respectively; these were not significantly different compared with controls (30.4 ± 0.8 mm and 46.5 ± 0.3 mm, respectively). However, proximal epididymal regions I, II, and III of *Src*^{-/-} appeared smaller and underdeveloped compared with littermate controls (Fig. 6B). In controls, a high level of phospho-MAPK3/1 appeared in region I and extended to entire region II at P17 (Fig. 6, C and E).

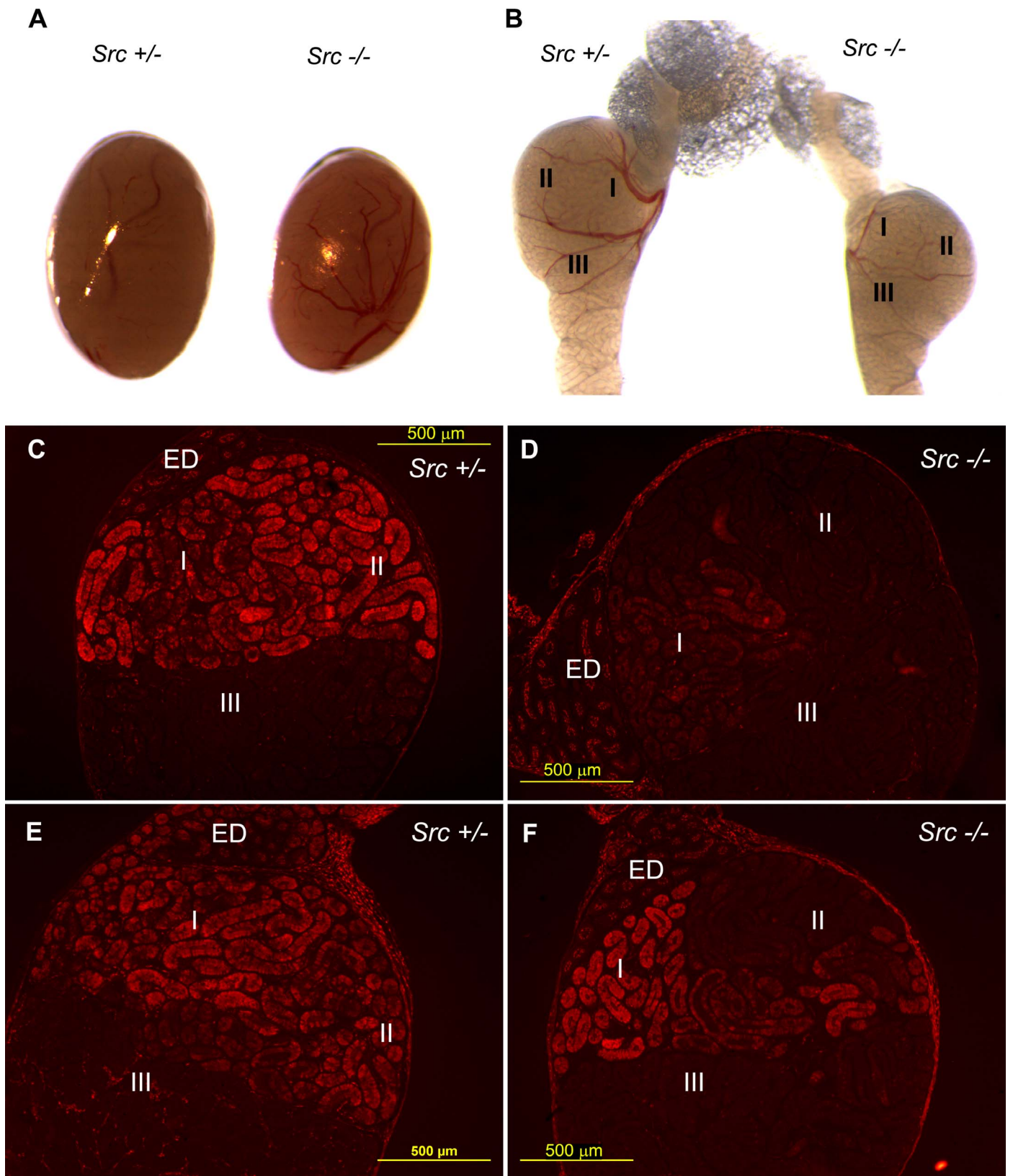


FIG. 6. A reduced initial segment size and reduced levels of phospho-MAPK3/1 following loss of *Src*. **A)** Testes from *Src*^{+/-} and *Src*^{-/-}. The testis size is comparable between controls and knockouts. **B)** Proximal epididymal regions (I, II, and III) from *Src*^{+/-} and *Src*^{-/-}. Epididymal regions I, II, and III of *Src*^{-/-} were smaller and underdeveloped compared with controls. **C-F)** Representative images of phospho-MAPK3/1 labeling in epididymal regions I, II, and III in *Src*^{+/-} (**C** and **E**) and *Src*^{-/-} (**D** and **F**) at P17. ED: efferent ducts.

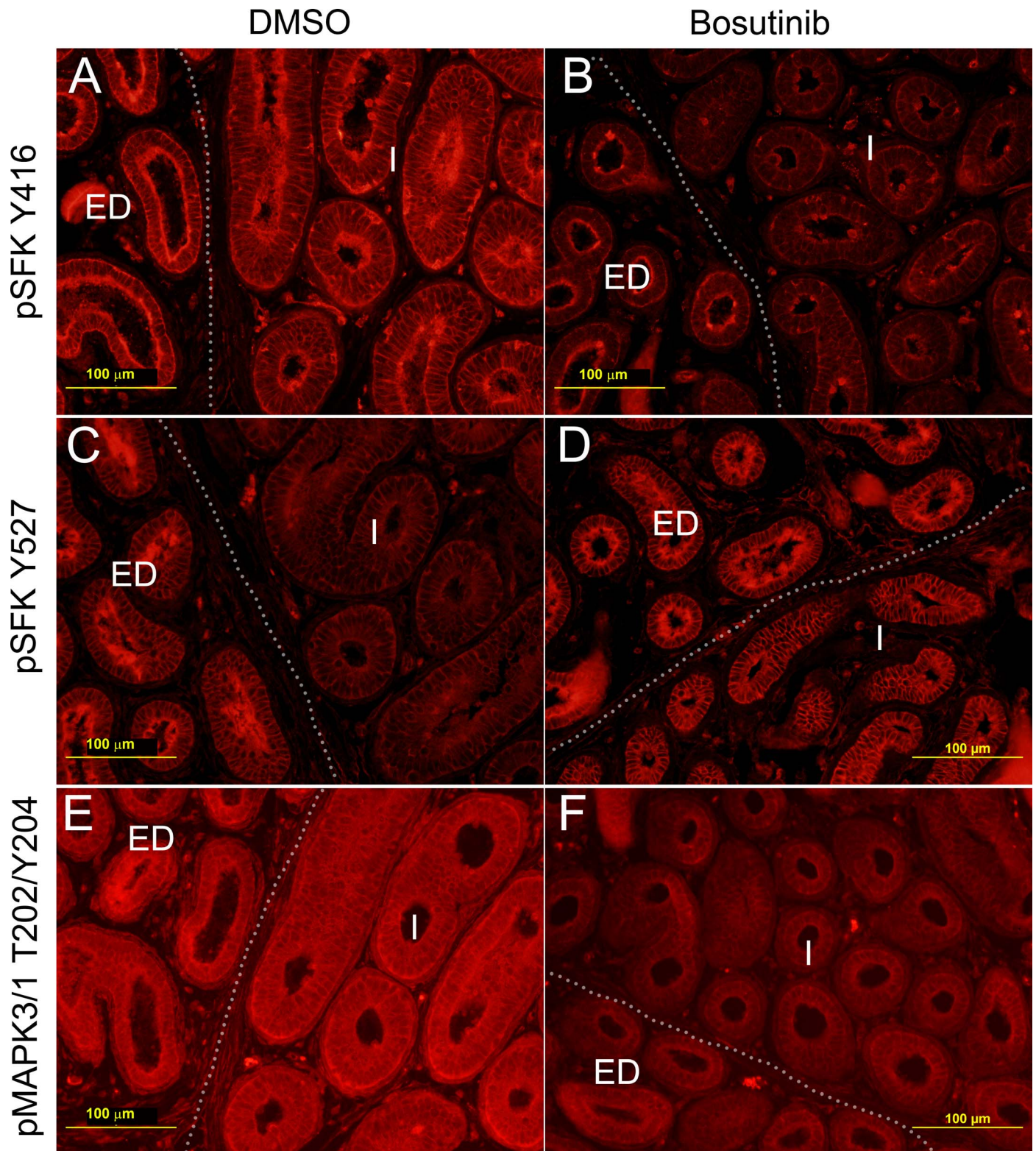


FIG. 7. A reduced level of SRC and MAPK3/1 activities following SRC inhibition. **A** and **B**) Comparison of phospho-SFK levels at Y416 in region I between control and treatment groups. **C** and **D**) Comparison of phospho-SFK levels at Y527 in region I between control and treatment groups. **E** and **F**) Comparison of MAPK3/1 activities in region I between control and treatment groups. ED: efferent ducts. The dotted lines show the border between region I and ED.

However, in knockouts, only a small area of region I closest to the efferent ducts displayed the high level of phospho-MAPK3/

1 (Fig. 6D), or the high level of phospho-MAPK3/1 was present in region I but did not extend to region II at P17 (Fig. 6F).

Inhibition of SRC Affected Initial Segment Differentiation as Measured by Changes in Phospho-MAPK3/1

Bosutinib, a bioavailable SRC inhibitor (code name SKI-606) [15] was administered daily to mice from P15 to P19. Figure 7, A–D, shows that SRC activity levels declined upon inhibitor treatment. The levels of SRC phosphorylated at the activation site Y416 were lower in initial segment region I of treated mice compared with DMSO controls (Fig. 7, A and B), whereas the levels of SRC phosphorylated at the inhibitory site Y527 were higher in treated mice compared with controls (Fig. 7, C and D). Phospho-MAPK3/1 levels were lower in initial segment region I of treated mice compared with controls (Fig. 7, E and F).

DISCUSSION

The first stage of epididymal postnatal development, prior to P15 in the mouse, is referred to as the undifferentiated period. During this stage, initial segment epithelial cells were never exposed to lumicrine factors. It is not surprising that undifferentiated epithelial cells do not depend on lumicrine factors for cell proliferation and survival. In contrast, during the second stage, from P15 to P19, initial segment epithelial cells responded to the first wave of lumicrine factors and established lumicrine factor dependency. Simultaneously, initial segment differentiation began, and the initial segment-specific kinase activity profile was established. Therefore, we referred to P15 to P19 as a critical window of initiation of initial segment differentiation. During the third stage, from P19 to P44, initial segment epithelial cells continued their differentiation processes. Different cell types—basal cells, principal cells, narrow cells, and clear cells—appeared from P28 onward [2]. Epithelial cells undergoing differentiation relied on lumicrine factors for both proliferation and survival (Fig. 1). This period was referred to as the period of initial segment differentiation. During the fourth stage, from 6 wk onward, cell proliferation of differentiated cells was very low, but already differentiated cells in the initial segment relied on lumicrine factors for survival (Fig. 1) [9, 16]. We referred to this stage as the differentiated period. Taken together, initial segment epithelial cells undergo each differentiation stage during postnatal development, and they respond to the exposure of lumicrine factors differently at each stage.

The SFK, ERK, and AMPK pathway components responded to lumicrine factors soon after they entered the epididymal duct. In contrast, PTEN, MET, and EGFR established the initial segment-specific expression/activity pattern much later, at approximately P28 (Fig. 5). Therefore, we hypothesized that the early response proteins were likely involved in initiation of initial segment differentiation. The late response proteins likely reflected the characteristics of a differentiated initial segment, and played roles in the maintenance of initial segment differentiation. This hypothesis was consistent with our previous report, in which we showed that a high activity level of PTEN in the initial segment sustained a high activity level of the ERK pathway, which in turn maintained initial segment differentiation [7].

The identity of lumicrine factors is not known. Multiple growth factors, including fibroblast growth factors, and high levels of androgen and androgen-binding protein were detected in luminal fluid [2, 17, 18]. It was hypothesized that growth factors regulated permissive signal pathways, whereas nongenomic actions of AR enhanced signal transduction regulation [17–20]. It was also demonstrated that multiple signal pathways responded to the entry or deprivation of lumicrine

factors in the initial segment [16, 21]. Among them, the ERK pathway rapidly and intensively responded to the changes in lumicrine factors [9, 16]. We previously revealed that MAP2K1/2 and MAPK3/1 activities were affected by the changes of lumicrine factors [9, 16]. In this report, we showed that RAF1, another component of the RAF/MEK/ERK signal cascade, had increased activity upon lumicrine factor exposure. It was also possible that the increased activity or expression levels of RPS6, CCND1, and the AMPK pathway components from P15 to P19 were the result of upregulation of the ERK pathway because these signal molecules were known to interact with the ERK pathway [22, 23]. It is likely that the ERK pathway is in the center of multiple lumicrine-regulated signal transduction pathways.

Several knockout animal models revealed that the high activity levels of the ERK pathway were essential for initial segment differentiation, and therefore for male fertility. A recent study using *Ros1* knockouts showed that loss of *Ros1* or pharmacological inhibition of ROS1 resulted in a decrease in the activity levels of the ERK pathway, and in turn loss of initial segment differentiation and male fertility [24]. In initial segment-specific *Pten* knockouts, activated AKT (thymoma viral proto-oncogene) suppressed the RAF1/ERK pathway, which eventually resulted in dedifferentiation of the initial segment and male infertility [7]. In initial segment-specific *Ar* knockouts, the activity levels of the ERK pathway components were reduced. Subsequently, impairment of initial segment differentiation and male infertility were observed [19]. Consistently, in vitro experiments showed that androgen regulated the ERK pathway through the nongenomic action of AR [18]. Therefore, the high activity level of the ERK pathway is a driving force of initial segment differentiation and is required for male fertility.

Notably, AR protein levels did not change from P15 to P19 (Fig. 3). *Ar* mRNA levels were not significantly reduced following the deprivation of lumicrine factors [16]. Therefore, it is unlikely that lumicrine factors regulated genomic actions of AR through transcriptional regulation.

In addition to the ERK pathway components, we found that SFK was another key signaling molecule in lumicrine regulation. SFK activity levels responded rapidly to the exposure or loss of lumicrine factors (Fig. 2) [9]. It is well known that SFK can regulate cellular function via the ERK pathway [25]. Consistently, in this study, we showed that deletion of *Src* gene and pharmacological inhibition of SRC activity both resulted in a decrease of MAPK3/1 activity. Therefore, we hypothesize that SRC signaling through the ERK pathway regulates initial segment differentiation.

SFK is a family of nine members, with SRC being abundant in many tissues [25]. It has been suggested that other members of SFK might compensate for SRC function in *Src* null mice [11]. Loss of *Src* reduced but did not abolish the high MAPK3/1 activities in the initial segment epithelium. Suppression of SRC activity by an inhibitor had stronger inhibitory effects on MAPK3/1 activities, but it also did not completely diminish the high MAPK3/1 activities in the initial segment. Likely, several SFK family members, rather than a single member, regulated MAPK3/1 activities and initial segment differentiation.

In summary, we discovered that the development of mouse initial segment from P15 to P19 was a critical window in which the SFK/ERK/AMPK signaling pathways rapidly responded to lumicrine factors, which in turn initiated differentiation of this epididymal region. In addition, this study provided evidence that SRC signaling through the ERK pathway played a major role during the initiation of initial segment differentiation.

Differentiation of this epididymal region is crucial for male fertility [5–7, 24].

ACKNOWLEDGMENT

We thank Chirag Y. Patel for his assistance in performing experiments. We thank Dr. Jonathan A. Cooper for providing us with *Src*^{+/-} mice.

REFERENCES

- Hinton BT, Galdamez MM, Sutherland A, Bomgardner D, Xu B, Abdel-Fattah R, Yang L. How do you get six meters of epididymis inside a human scrotum? *J Androl* 2011; 32:558–564.
- Robaire B, Hinton BT. The epididymis. In: Plant T, Zeleznik AJ (eds.), Knobil and Neill's Physiology of Reproduction, 4th ed. New York: Elsevier; 2014:691–772.
- Jelinsky SA, Turner TT, Bang HJ, Finger JN, Solarz MK, Wilson E, Brown EL, Kopf GS, Johnston DS. The rat epididymal transcriptome: comparison of segmental gene expression in the rat and mouse epididymides. *Biol Reprod* 2007; 76:561–570.
- Johnston DS, Turner TT, Finger JN, Owtsharuk TL, Kopf GS, Jelinsky SA. Identification of epididymis-specific transcripts in the mouse and rat by transcriptional profiling. *Asian J Androl* 2007; 9:522–527.
- Sonnenberg-Riethmacher E, Walter B, Riethmacher D, Godecke S, Birchmeier C. The c-ros tyrosine kinase receptor controls regionalization and differentiation of epithelial cells in the epididymis. *Genes Dev* 1996; 10:1184–1193.
- Yeung CH, Sonnenberg-Riethmacher E, Cooper TG. Infertile spermatozoa of c-ros tyrosine kinase receptor knockout mice show flagellar angulation and maturational defects in cell volume regulatory mechanisms. *Biol Reprod* 1999; 61:1062–1069.
- Xu BF, Washington AM, Hinton BT. PTEN signaling through RAF1 proto-oncogene serine/threonine kinase (RAF1)/ERK in the epididymis is essential for male fertility. *Proc Natl Acad Sci U S A* 2014; 111:18643–18648.
- Jegou B, Le Gac F, de Kretser DM. Seminiferous tubule fluid and interstitial fluid production, I: effects of age and hormonal regulation in immature rats. *Biol Reprod* 1982; 27:590–595.
- Xu B, Yang L, Lye RJ, Hinton BT. p-MAPK1/3 and DUSP6 regulate epididymal cell proliferation and survival in a region-specific manner in mice. *Biol Reprod* 2010; 83:807–817.
- Johnston DS, Jelinsky SA, Bang HJ, DiCandeloro P, Wilson E, Kopf GS, Turner TT. The mouse epididymal transcriptome: transcriptional profiling of segmental gene expression in the epididymis. *Biol Reprod* 2005; 73:404–413.
- Soriano P, Montgomery C, Geske R, Bradley A. Targeted disruption of the c-src proto-oncogene leads to osteopetrosis in mice. *Cell* 1991; 64:693–702.
- Krapf D, Ruan YC, Wertheimer EV, Battistone MA, Pawlak JB, Sanjay A, Pilder SH, Cuasnicu P, Breton S, Visconti PE. cSrc is necessary for epididymal development and is incorporated into sperm during epididymal transit. *Dev Biol* 2012; 369:43–53.
- Palladino MA, Hinton BT. Expression of multiple gamma-glutamyl transpeptidase messenger ribonucleic acid transcripts in the adult rat epididymis is differentially regulated by androgens and testicular factors in a region-specific manner. *Endocrinology* 1994; 135:1146–1156.
- Xu W, Harrison SC, Eck MJ. Three-dimensional structure of the tyrosine kinase c-Src. *Nature* 1997; 385:595–602.
- Amsberg GK, Koschmieder S. Profile of bosutinib and its clinical potential in the treatment of chronic myeloid leukemia. *Onco Targets Ther* 2013; 6:99–106.
- Xu B, Abdel-Fattah R, Yang L, Crenshaw SA, Black MB, Hinton BT. Testicular lumicrine factors regulate ERK, STAT, and NFkB pathways in the initial segment of the rat epididymis to prevent apoptosis. *Biol Reprod* 2011; 84:1282–1291.
- Lan ZJ, Labus JC, Hinton BT. Regulation of gamma-glutamyl transpeptidase catalytic activity and protein level in the initial segment of the rat epididymis by testicular factors: role of basic fibroblast growth factor. *Biol Reprod* 1998; 58:197–206.
- Hamzeh M, Robaire B. Androgens activate mitogen-activated protein kinase via epidermal growth factor receptor/insulin-like growth factor 1 receptor in the mouse PC-1 cell line. *J Endocrinol* 2011; 209:55–64.
- Krutsikh A, De Gendt K, Sharp V, Verhoeven G, Poutanen M, Huhtaniemi I. Targeted inactivation of the androgen receptor gene in murine proximal epididymis causes epithelial hypotrophy and obstructive azoospermia. *Endocrinology* 2011; 152:689–696.
- Xu B, Yang L, Hinton BT. The role of fibroblast growth factor receptor substrate 2 (FRS2) in the regulation of two activity levels of the components of the extracellular signal-regulated kinase (ERK) pathway in the mouse epididymis. *Biol Reprod* 2013; 89:1–13.
- Turner TT, Johnston DS, Finger JN, Jelinsky SA. Differential gene expression among the proximal segments of the rat epididymis is lost after efferent duct ligation. *Biol Reprod* 2007; 77:165–171.
- Lopez-Cotarelo P, Escribano-Diaz C, Gonzalez-Bethencourt IL, Gomez-Moreira C, Deguiz ML, Torres-Bacete J, Gomez-Cabanas L, Fernandez-Barrera J, Delgado-Martin C, Mellado M, Regueiro JR, Miranda-Carus ME, et al. A novel MEK-ERK-AMPK signaling axis controls chemokine receptor CCR7-dependent survival in human mature dendritic cells. *J Biol Chem* 2015; 290:827–840.
- Eisinger-Mathason TS, Andrade J, Lannigan DA. RSK in tumorigenesis: connections to steroid signaling. *Steroids* 2010; 75:191–202.
- Jun HJ, Roy J, Smith TB, Wood LB, Lane K, Woolfenden S, Punko D, Bronson RT, Haigis KM, Breton S, Charest A. ROS1 signaling regulates epithelial differentiation in the epididymis. *Endocrinology* 2014; 155:3661–3673.
- Kim LC, Song L, Haura EB. Src kinases as therapeutic targets for cancer. *Nat Rev Clin Oncol* 2009; 6:587–595.